

### EXAMPLE PROBLEM 3.3.3.3

## THE EFFECTS OF RIVET YIELDING ON RESIDUAL STRENGTH OF STIFFENED STRUCTURE CONTAINING CRACKS

T. Swift

McDonnell Douglas Corporation  
(Literal)

### 1. INTRODUCTION

The residual strength of a riveted structure containing cracks can be determined using elastic finite element methods. These methods have been shown to give reasonable results when the skin material fracture toughness is comparatively low [1]. In these methods, the simulation of rivet flexibility is essential to obtain reasonable analysis-test correlation. When material fracture toughness is high and when the crack tips extend beyond the crack arresting stiffeners, it is often necessary to consider nonlinear shear displacement characteristics of the rivets. If this is not considered, one can easily be misled by the elastic analysis results. Certain difficulties exist with non-linear finite element analyses. These difficulties are mainly associated with computer operational costs. Displacement compatibility methods offer considerable reductions in computer running time and the use of this approach together with non-linear fastener displacement characteristics becomes economically feasible. This example briefly describes just such an analysis which correlated with testing extremely well.

### 2. STATEMENT OF THE PROBLEM

During the development test phase of a large transport aircraft, a stiffened panel containing a 2 bay skin crack with a saw cut central stiffener, was tested for its residual strength. The panel, measuring 120 inches long by 60 inches wide, was made from 2024-T3 sheet 0.071 inches thick. Stiffeners, spaced at 8 inches, were made from "hat" section 7075-T6 extrusions, 0.5471 square inches in cross-sectional area. A skin crack was propagated into two skin bays, normal to the longitudinal stiffening and equally spaced about a central saw-cut stiffener. Static loading was applied to failure after the skin crack tips had propagated beyond the crack arresting adjacent stiffener.

Failure of the panel was precipitated by rivet failure over the entire length of the crack arresting stiffener at a gross area stress of 39.7 ksi with a half crack length of 9.88 inches. Elastic finite element analysis would predict the failure mode as being rivet critical but the allowable gross stress at failure would be too low by a factor of 3.5 to 1. This analysis indicates that the load in the first rivet, adjacent to the crack in the crack arresting stiffener, is extremely high. In fact, considerable non-linear displacement of this rivet occurs causing adjacent rivets, progressively further away from the crack, to accept more load. When this occurs the stiffener becomes less effective in reducing the crack tip stress intensity factor and the panel gross allowable stress, from a skin fracture standpoint, is reduced. This effect, of course, cannot be assessed by elastic analysis.

### 3. ANALYSIS

The analysis used to correlate the results of the panel test was based on the displacement compatibility method. The details of this method are presented in the literature [2]. Figure 1 illustrates the method and as can be seen from the figure, either adhesively bonded or riveted structures can be considered. Correlation of an adhesively bonded test panel, using this approach, appears in the literature [3]. The approach is based on equating displacements in the cracked sheet with displacements in the stiffening elements after taking account of fastening system flexibility. Displacements in the cracked sheet are calculated at discrete points using the Westergaard Complex Stress Function approach. Fastening system flexibility and stiffener bending are both accounted for. The number of effective rivets on each side of the crack in each stiffener is usually 15. This was determined by obtaining solutions with different number of effective rivets assumed and then plotting crack tip stress intensity factor as a function of number of effective rivets. This plot becomes asymptotic at approximately 15 rivets for the 2 bay crack case with a broken central stiffener. A matrix of influence coefficients is inverted to obtain all the rivet loads. Crack tip stress intensity factor in the sheet is then determined from Muskhelishvili's methods [4]. The elastic-plastic load displacement characteristics, obtained from simple lap splice tests, was simulated by the tri-elastic model shown in Figure 2 for the test panel under consideration. The computer program, developed for this case, first generates an elastic solution based on the elastic slope of the rivet load displacement curve. All rivet loads are then compared to the tri-elastic model and the rivet flexibility matrix is then re-generated and a second solution produced. This procedure continues until the crack tip stress intensity factor difference between successive iterations is less than a specified value. The final stress intensity factor, for the specific applied gross area stress and crack size, is printed out together with all rivet loads and stiffener stresses.

### 4. ANALYSIS RESULTS

The analysis results for the first elastic iteration of the test panel configuration are shown in Figure 3. The skin fracture curve is plotted using 8 values (see analysis in example 3.3.3.1) obtained from the program together with a skin fracture toughness value  $K_{IC}$  of 197.87 ksi  $\sqrt{\text{in}}$ , obtained from fast fracture of a previously tested stiffened panel of different configuration from the one considered here. At the failure half crack length of 9.88 inches, it can be seen from Figure 3 that the gross allowable stresses are 11.5 ksi, 32.5 ksi and 53.6 ksi from rivet failure, stiffener failure and skin fracture criteria respectively. Actual failure took place at 39.7 ksi. It can be seen therefore that one could be misled by the results of an elastic analysis. The elastic-plastic computer program has the ability to consider the effects of rivet failure and Figure 4 shows rivet displacement as a function of gross area stress for various number of rivets failed starting adjacent to the crack. As can be seen from the figure there is considerable difference between elastic and plastic solutions. With all the rivets intact the first rivet yields at a gross area stress of only 6.806 ksi. Yielding continues as the gross area stress is increased until point J is reached on line CD, when failure of the first rivet occurs.

Line CD represents the average failure displacement of the rivet. Lines AB and EF represent lower and upper bounds of rivet failure displacement respectively. The crack tip stress intensity factor as a function of gross area stress is shown in Figure 5. The upper curve considers that all rivets are intact and the other curves are for different number of rivets failed. When the first rivet fails at constant gross area stress the stress intensity factor increases as can be seen in Figure 5. The vertical line AB represents the critical stress intensity factor of 197.87 ksi  $\sqrt{\text{in.}}$ , obtained from a previous test. The vertical line CD represents a  $K_{IC}$  value of 215 ksi  $\sqrt{\text{in.}}$  used for illustration purposes later.

Figure 6 shows a cross plot of the intersection of vertical line CD of Figure 4 with the rivet displacement curves. This cross plot is titled Rivet Failure Curve. Similarly, vertical lines AB and CD of Figure 5 are cross plotted in Figure 6 and are titled Skin Fracture Curve  $K_{IC} = 197.87$  ksi  $\sqrt{\text{in.}}$  and Skin Fracture Curve  $K_{IC} = 215$  ksi  $\sqrt{\text{in.}}$  respectively. Figure 6 represents a residual strength diagram for a half crack length of 9.88 inches. To illustrate how this diagram works, assume for the time being that the skin fracture toughness  $K_{IC} = 215$  ksi  $\sqrt{\text{in.}}$ . Loading is applied slowly and the first rivet adjacent to the crack fails at point A of Figure 6 corresponding to gross area stress of 39.5 ksi. The panel allowable from a skin fracture standpoint immediately drops from point B to C. Total failure does not however take place because the panel allowable based on second rivet failure has increased to point D since this rivet is further away from the crack and therefore less critical. The load is still only at 39.5 ksi represented by point B and therefore lower than C or D. Total panel failure would now occur if the load is increased to point C due to skin fracture. In the case of the panel under discussion the fracture toughness  $K_{IC}$  is only 197.87 ksi  $\sqrt{\text{in.}}$ . When the first rivet fails at 39.5 ksi gross stress, represented by point A of Figure 6, the entire panel fails due to fracture instability in the skin, since the panel allowable from a skin fracture standpoint drops from point F to point G, which is below the applied stress. This value is less than 1% lower than the actual panel failure stress of 39.74 ksi. Variation in rivet failure displacement, represented by the lower bound line AB and the upper bound line EF of Figure 4, would give variation of panel failure between points G and F of Figure 6. The explanation here is that at the lower bound point G of Figure 4, failure of the first rivet would occur at 37.5 ksi. This is lower than point C of Figure 6 so the load could be increased to 39 ksi, represented by point G of Figure 6. Consider the upper bound point H of Figure 4, where the first rivet would fail at 42 ksi. In this case the panel failure stress would be limited to 41 ksi represented by point F of Figure 6. This then represents a spread in allowable between 39.0 and 41.0 ksi equivalent to minus 1.86 and plus 3.17 per cent of the actual failure stress.

#### 5. CONCLUSIONS

It has been shown that when crack tips extend beyond the crack arresting stiffeners of a panel containing a two bay crack that elastic analysis will not predict the true gross stress at failure. For the configuration discussed, consideration of the elastic-plastic rivet load-displacement characteristics gave excellent correlation with test results. This elastic-plastic analysis was made economically feasible with the displacement compatibility method whereas non-linear finite element methods would have been extremely costly.

#### 6. REFERENCES

1. Swift, T. and Wang, D.Y., "Damage Tolerance Design-Analysis Methods and Test Verification of Fuselage Structure", *AFDL-TR-70-144*, 1970.
2. Swift, T., "The Effects of Fastener Flexibility and Stiffener Geometry on the Stress Intensity in Stiffened Cracked Sheet", published in "Prospects of Fracture Mechanics", Noordhoff International Publishing, Leyden, Netherlands.
3. Swift, T., "Fracture Analysis of Adhesively Bonded Cracked Panels", *TRANS. ASME Journal of Engineering Materials and Technology*, Jan. 1978.
4. Paris, P.C., "Application of Muskhelishvili's Intensity Factors for Plane Problems, Part III, Lehigh University, 1960.

#### 7. COMMENTARY

This is an excellent example of the application of fracture mechanics techniques to predict the behaviour of stiffened panels as a function of applied load. By performing analytical studies as described in this example, even during the design stage of an aircraft the designer can find out which structural elements will precipitate failure. If the results do not meet his requirements, on the basis of such an analysis he is able to modify his design. Finally, this example clearly demonstrates that on the basis of purely elastic computations one may easily come to wrong conclusions when the prediction of residual strength behaviour of a structure is involved. In this respect analytical methods are preferable to finite element methods because yielding of one or more elements can easily be incorporated in the computation procedure.

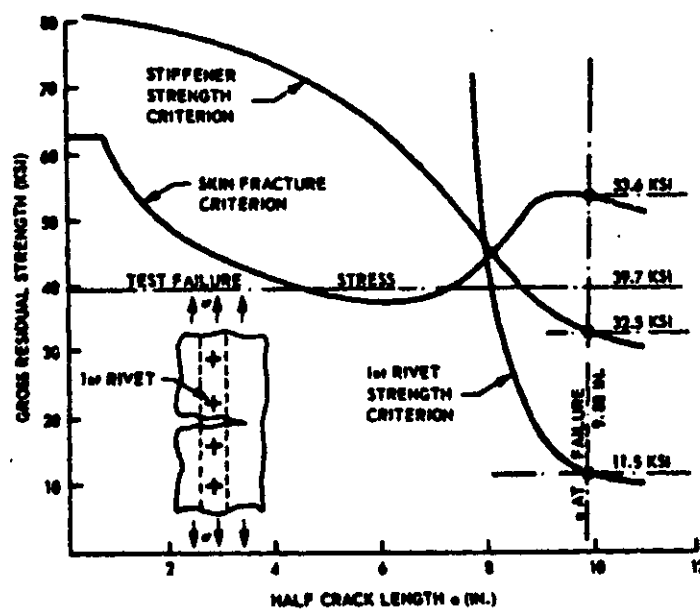


FIGURE 3 RESIDUAL STRENGTH DIAGRAM-ELASTIC ANALYSIS RESULTS

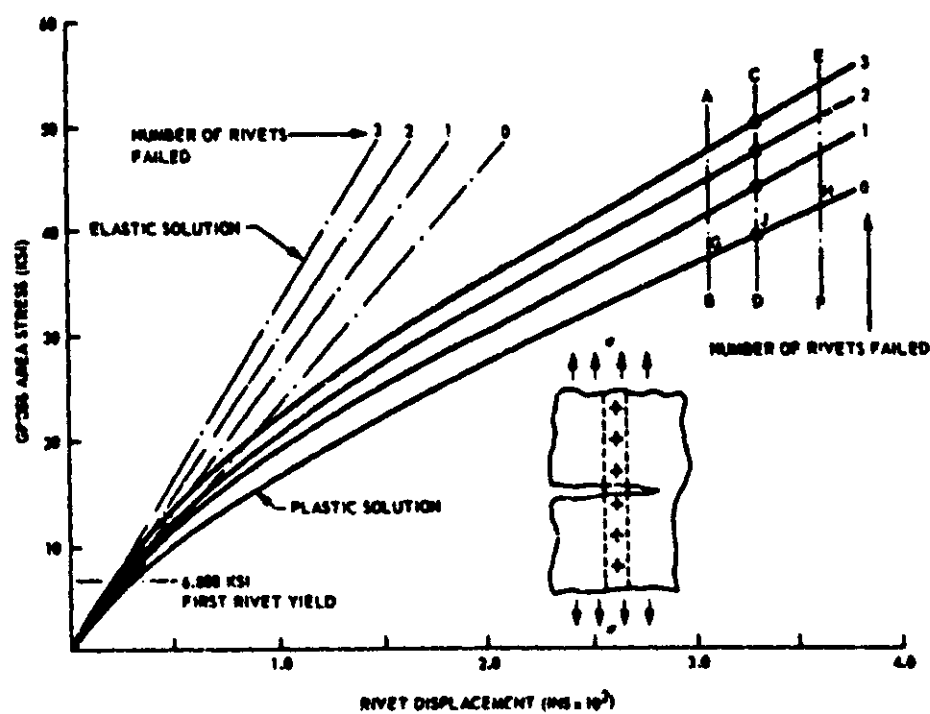


FIGURE 4 RIVET DISPLACEMENT AS A FUNCTION OF GROSS AREA STRESS (HALF CRACK LENGTH 9.88 INCHES)

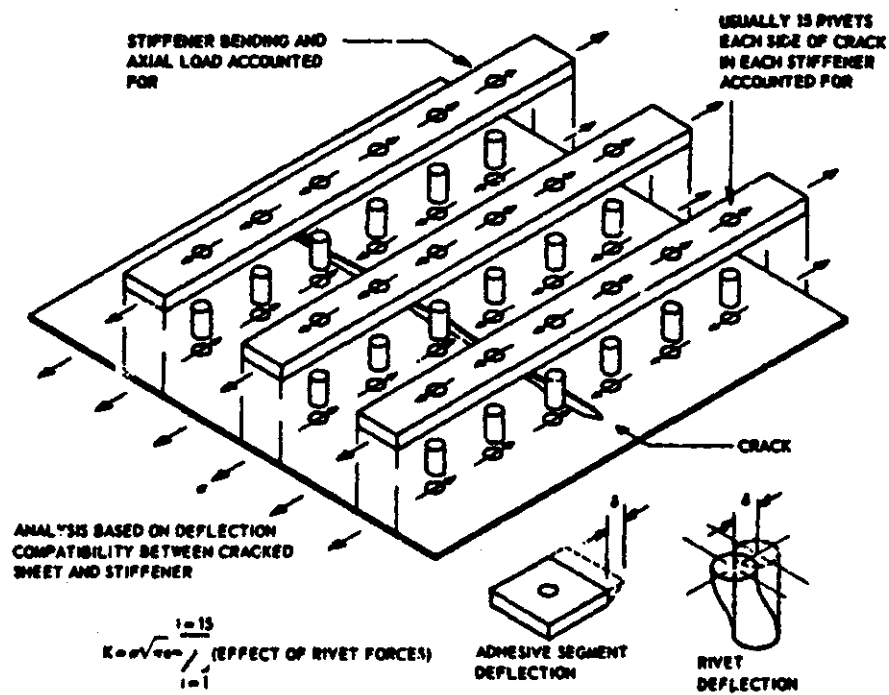


FIGURE 1 DISPLACEMENT COMPATIBILITY METHOD FOR FRACTURE ANALYSIS

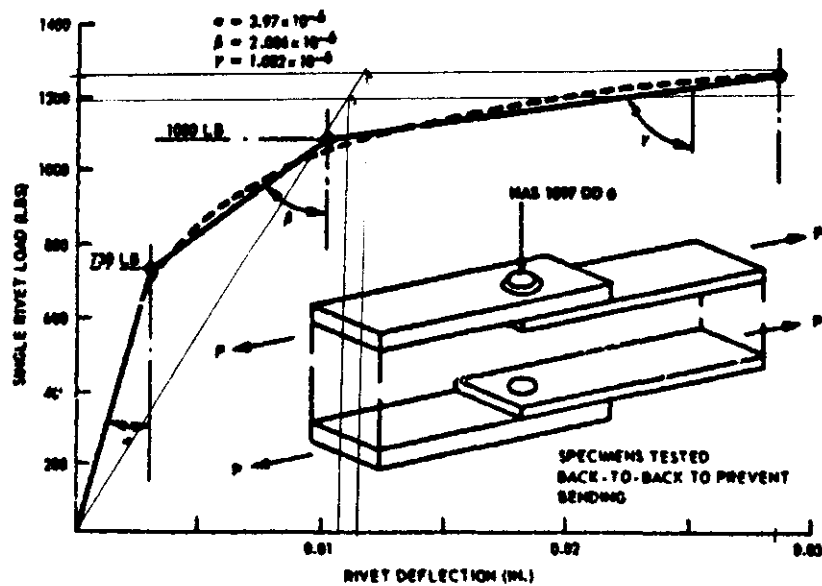


FIGURE 2 TRI-ELASTO-PLASTIC MODEL FOR RIVET LOAD DISPLACEMENT

$$0.254 \times 5000 = 20.000$$

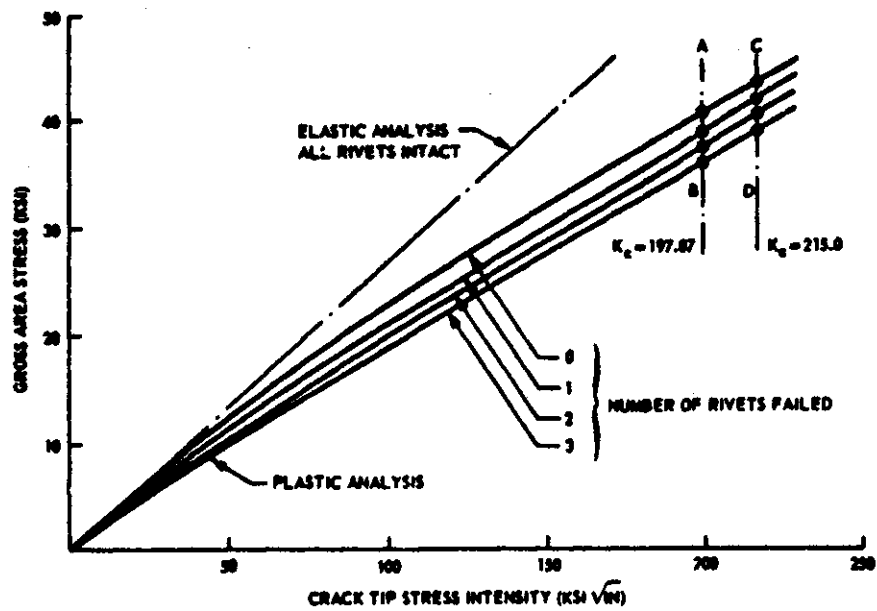


FIGURE 5 CRACK TIP STRESS INTENSITY FACTOR VERSUS GROSS AREA STRESS (HALF CRACK LENGTH 9.88 INCHES)

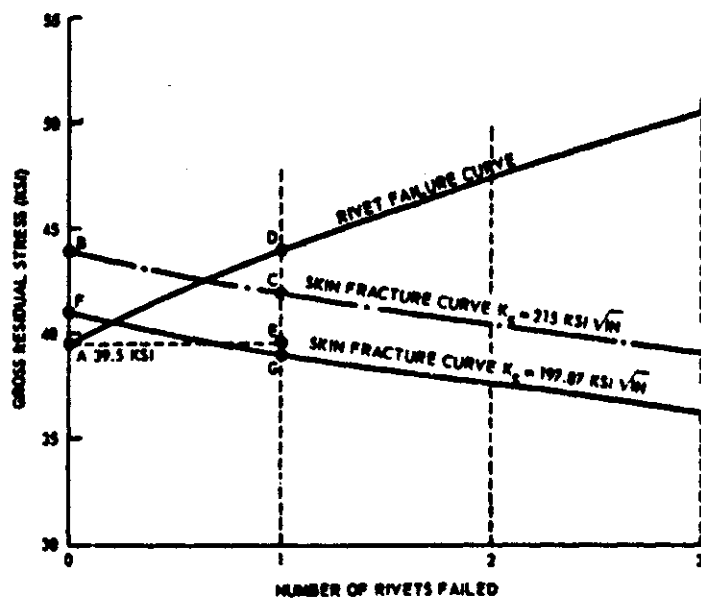


FIGURE 6 RESIDUAL STRENGTH DIAGRAM-HALF CRACK LENGTH 9.88 INCHES